ACS OMEGA

http://pubs.acs.org/journal/acsodf

Article

In Vitro and *In Silico* Study to Assess Toxic Mechanisms of Hybrid Molecules of Quinone-Benzocaine as Plastoquinone Analogues in Breast Cancer Cells

Ayse Mine Yilmaz Goler,◆ Ayse Tarbin Jannuzzi,◆ Nilüfer Bayrak, Mahmut Yıldız, Hatice Yıldırım, Masami Otsuka, Mikako Fujita, Mohamed O. Radwan, and Amaç Fatih TuYuN*

Cite This: *ACS Omega* 2022, 7, 30250−30264

Read Online

ACCESS | Metrics & More | Article Recommendations | Supporting Information

ABSTRACT: We managed to obtain three different series of 2,3-dimethyl-1,4-benzoquinones, named nonhalogenated and halogenated (brominated and chlorinated) PQ analogues, *via* the molecular hybridization strategy. Sixteen of eighteen hybrid molecules were selected by the National Cancer Institute (NCI) of Bethesda for their *in vitro* antiproliferative potential against the full NCI 60 cell line panel. The hybrid molecules (**BrPQ5**, **CIPQ1**, and **CIPQ3**) showed good growth inhibition at 10 μM concentration, particularly against breast cancer cell lines. As per the results obtained from *in vitro* antiproliferative evaluation, cytotoxic activities of the hybrid molecules (**BrPQ5**, **CIPQ1**, and **CIPQ3**) were evaluated with an 3-(4,5-dimethylthiazol-2-yl)-2,5-diphenyltetrazolium bromide (MTT) assay in T47D and MCF7 breast cancer and human umbilical vein endothelial (HUVEC) cells. Molecules exhibited cytotoxic activity, and especially, **CIPQ1** showed remarkable cytotoxic activity and good selectivity on T47D and MCF7 cells. Furthermore, **CIPQ1** could inhibit cell proliferation, cause apoptotic cell death and disturb the cell cycle in T47D and MCF7 cells. Additionally, **CIPQ1** caused oxidative stress induction in both cells, more so in T47D. *In vitro* study results indicated that the anticancer activity of **CIPQ1** was more prominent in T47D cells than in MCF7 cells. The compound **CIPQ1** showed a prominent binding with JNK3 *in silico*. Thus, the obtained hybrid molecules *via* the molecular hybridization strategy of two important pharmacophores could be useful in the discovery of novel antiproliferative agents, and **CIPQ1** could be considered a promising drug candidate.

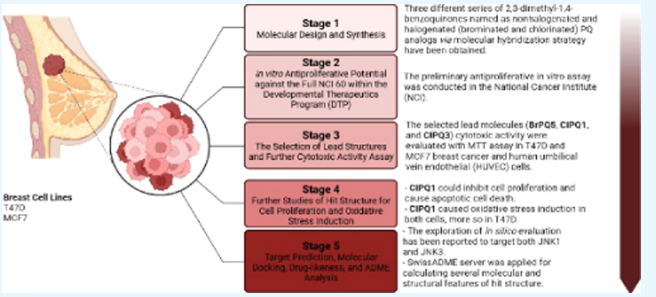

1. INTRODUCTION

Proliferative diseases are expected to be the leading cause of death threatening the human race.[1,2] The discovery of chemotherapeutic agents for the pain relief and treatment of diseases has paved the way for modern medical practice. Over the centuries, crude extracts or dried parts of plants and natural products have been sources of medicines. Additionally, natural products can be identified as a treasure chest of prevalidated molecules.[3] Almost three out of four novel antiproliferative agents are derived from natural products and natural product-derived molecules. Such molecules obtained naturally might also avoid some side effects associated with synthetic drugs.[1,4] The discovery of prontosil in the 1930s by Gerhard Domagk and penicillin in 1928 by Alexander Fleming was a pioneer in the discovery and development of modern medicine.[5] Prior to the discovery of antibiotics, infectious diseases were the biggest problem in human history.[6] But, nowadays, the primary disease that has become a problem for humanity is cancer. Cancer has been the primary cause of 10 million deaths in 2020.[7] Commercialized drugs and drug leads (semisynthetic and/or synthetic) in the therapeutic treatment of infectious diseases and cancers come from natural products and natural product-derived molecules.[8] Modification of the moiety of the lead molecule is an attractive way to accelerate drug development processes as well as to further the discovery of promising agents in the chemotherapeutic field.[9]

A series of commercially available antiproliferative drugs like doxorubicin, idarubicin, and LY83583 consist of a 1,4-quinone moiety as a core structure.[10] For a long time in our laboratory, we have been searching for lead molecules based on natural products containing the quinone moiety. Recently, this moiety, especially containing two methyl groups or a pyridine, has been explored by synthesizing a series of novel molecules as both Plastoquinone[11,12] and LY83583 analogues[13] and evaluated for their antiproliferative activity against versatile cancer cell lines such as K-562 (myeloid leukemia), Jurkat, MT-2 (two other

Received: June 1, 2022
Accepted: August 2, 2022
Published: August 15, 2022

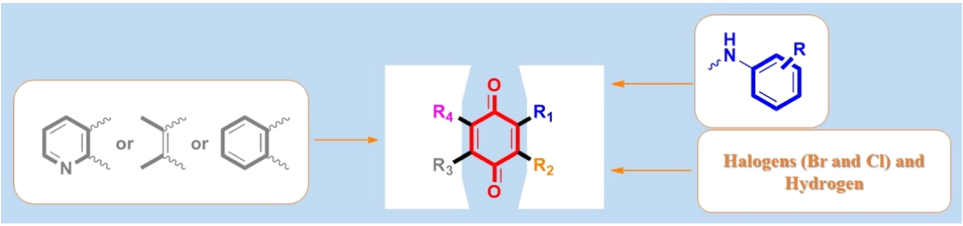

Figure 1. Scope of the target 1,4-quinones developed by modifications of the different substituent(s) in different positions.

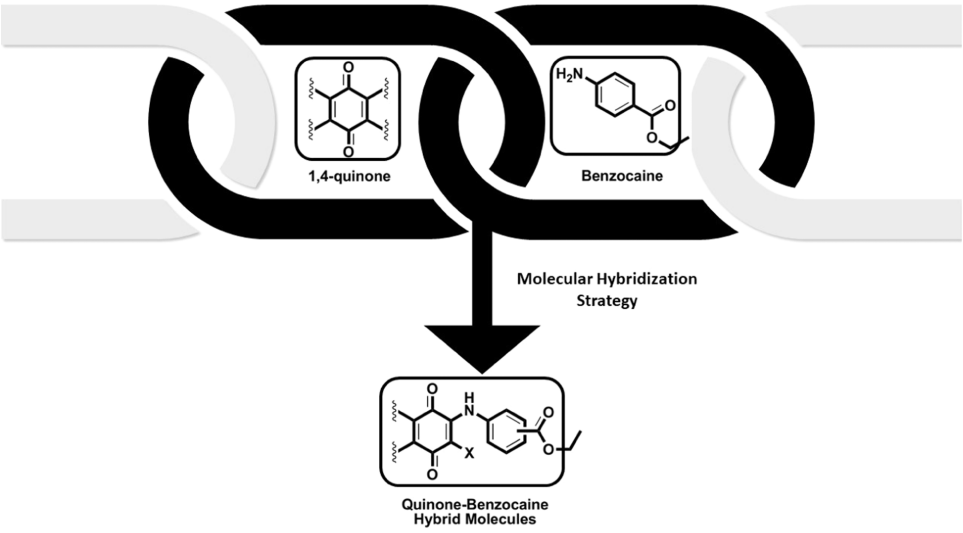

Figure 2. Molecular hybridization strategy to design the quinone-benzocaine hybrid molecules as Plastoquinone analogues with improved biological activities.

human T-cell leukemia), and HeLa cell lines (human cervical carcinoma). In most cases, various primary amines (aryl amine) have been introduced at the 2-position along with various substituent(s) modifications done at different positions of the aryl amine, as shown in Figure 1.

The molecular hybridization strategy, involving biologically active two or more pharmacophores, generates novel hybrid molecules with strong biological activities (Figure 2). Keeping in view the biological activities of 1,4-quinones and benzocaine,[14] the combination of these two important moieties could result in potential quinone-benzocaine hybrid molecules with improved biological activities.[15] Structural modifications of the hybrid molecules have led to promising leads in the chemotherapeutic field, and for that reason, it remains an attractive way to accelerate drug development processes.[16] In continuation of our earlier works[11,12] and an extension of our former work[17] aimed at finding the antimicrobial profile, the exploration of the *in vitro* antiproliferative activity of previously reported 2,3-dimethylquinone-benzocaine hybrid molecules as Plastoquinone analogues[17] *via* the molecular hybridization strategy along with *in silico* evaluation has been reported for the first time. In this series of quinone-benzocaine hybrid molecules, the structure−activity relationship (SAR) was evaluated by applying the aryl amine functionality at different positions of the phenyl ring through bioisosterism.

Breast cancer, a multifaced and complex disease, is based on the gene expression profile in one of its classifications. This classification divides tumor cells into Luminal A, Luminal B, Her2-enriched, and basal-like subtypes. Breast cancer treatment is selected depending on the classification of the tumor. It includes markers such as the proliferation factor (Ki67), epidermal growth factor (EGFR), and cytokeratin expression in addition to traditional marker expressions such as estrogen receptor (ER), progesterone receptor (PR), and epidermal growth receptor 2 (HER2).[18] In the treatment of Luminal A-type cancer, the most common type of breast cancer, the treatment approach is hormonal therapies alone or chemotherapy may be supplemented to the treatment. Although the recurrence rate is low in breast cancer, if it occurs, it is seen in the bone. Also, a high rate of resistance to treatments may develop.[19] Thus, the development of better choices for cancer chemotherapy is needed. In this study, we aimed to evaluate the potential anticancer effects of quinone-benzocaine hybrid molecules on breast cancer. Apoptosis is a selective process of physiological cell deletion that orchestrates cell replication/death balance. Uncontrolled cell-cycle progression and deregulation of apoptosis are two key features of cancer.[20] Hence, cell-cycle arrest and induction of apoptotic cancer cell death are deemed crucial approaches for the prevention and treatment of cancer. Consequently, many chemotherapeutics elicit their antitumor effects by induction of apoptosis in various cancer cells.[21] c-Jun N-terminal kinases (JNKs) are members of a family of important signal transduction enzymes known as mitogen-activated protein kinases (MAPKs). They can be activated by different stress factors.[22] A mountain of evidence indicated that JNKs play a pivotal role in the induction of apoptosis in human breast cancer cells and their signal transduction.[23] De facto, JNKs represent new and valid targets by therapeutic agents for the treatment of different diseases. Many JNK inhibitors based on different molecular scaffolds have been discovered in the past decade.[24]

https://doi.org/10.1021/acsomega.2c03428
ACS Omega 2022, 7, 30250−30264

Scheme 1. Synthesis of the Nonhalogenated (PQ1-6) and Halogenated PQ Analogues (BrPQ1-6 and ClPQ1-6)[a]

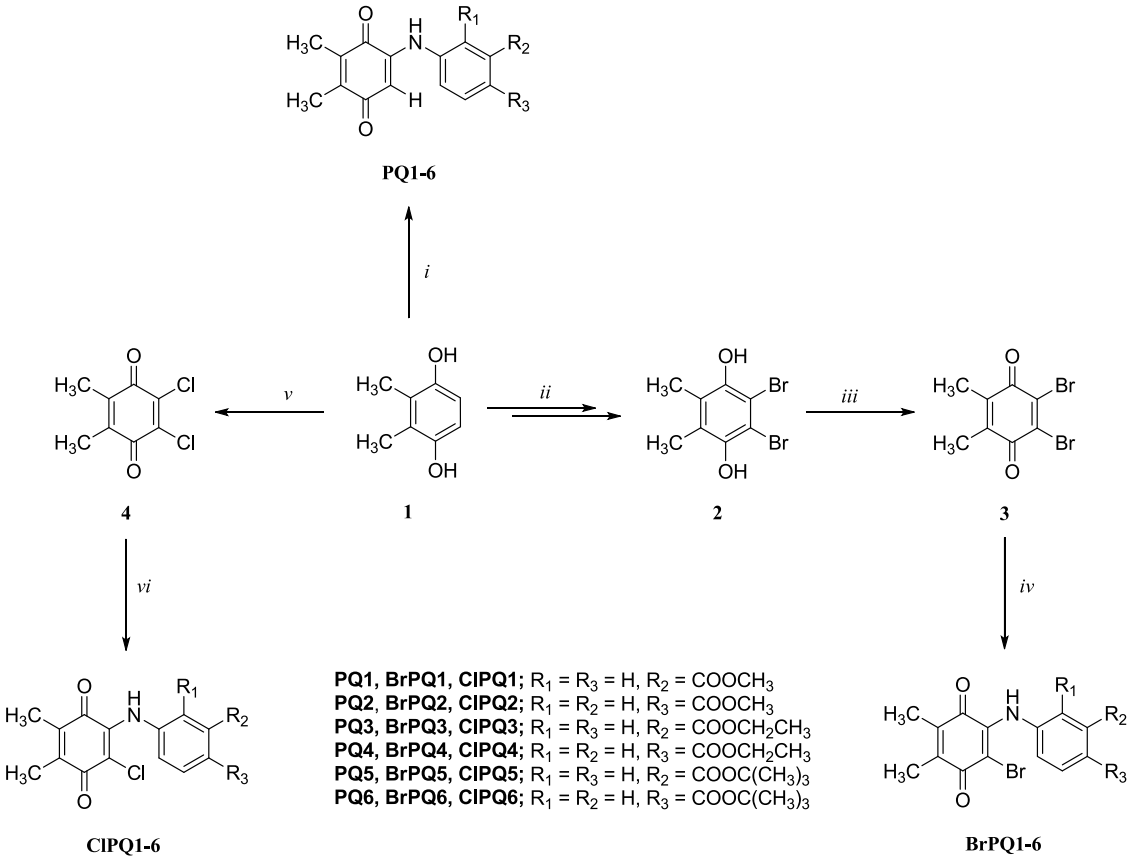

[a]Reagents and conditions: (i) Substituted amines, $NaIO_3$, H_2O/MeOH, rt, 12−24 h; (ii) Br_2, CH_3COOH,rt, 30 min in two steps; (iii) sodium hypochlorite (1.5% bleach); (iv) substituted amines, EtOH, rt, 8−16 h;(v) HNO_3/HCl, 10 min, 90 °C; (vi) substituted amines, EtOH, reflux, 8−16 h.

2. RESULTS AND DISCUSSION

2.1. Chemistry. In the search for new antiproliferative agents, the synthetic route used for the preparation of 2,3-dimethylquinone-benzocaine hybrid molecules as Plastoquinone analogues (PQ analogues) *via* the molecular hybridization strategy is outlined in Scheme 1. The routes of the nonhalogenated (**PQ1-6**) and halogenated PQ analogues (**BrPQ1-6** and **ClPQ1-6**) started from commercially available dimethylhydroquinone (**1**). First, the nonhalogenated PQ analogues (**PQ1-6**) were prepared from dimethylhydroquinone (**1**) and the corresponding substituted amine in the presence of an oxidizing agent ($NaIO_3$). The nonhalogenated PQ analogues (**PQ1-6**) was converted to the brominated PQ analogues (**BrPQ1-6**) by the reaction of the corresponding substituted amine and dibromobenzoquinone (**3**) using ethanol as the solvent (Scheme 1). Then, dichlorobenzoquinone (**4**) obtained from HNO_3/HCl variation at an elevated temperature was reacted with the corresponding substituted amine in reflux EtOH to form the chlorinated PQ analogues (**ClPQ1-6**). To reproduce PQ analogues, characterization details, complete results, and discussion of these analogues, kindly refer to our previous report.[17]

2.2. Biological Activities. *2.2.1. Preliminary In Vitro Antiproliferative Activity.* The preliminary *in vitro* antiproliferative assay was conducted in collaboration with the National Cancer Institute (NCI) of Bethesda within the Developmental Therapeutics Program (DTP) to explore the antiproliferative properties of the PQ analogues at a single dose of concentration (10 μM). It consists of a panel of 60 human cancer cell lines including nine tumor subpanels, namely, leukemia, lung, colon, CNS, melanoma, ovarian, renal, prostate, and breast cancer cell lines.[25] Prior to analysis, the purity of the hybrid PQ analogues was analyzed by HPLC (Shimadzu/DGU-20A5 HPLC apparatus fitted with a 25 cm Chiralpac AD-H chiral column) using hexane/2-propanol (95/5) as the mobile phase with a flow rate of 1.0 mL/min. The purity of all analogues was ≥95%. Their chromatograms are presented in the supplementary file as Figures SI 1−16. The main objective of NCI is to find the lead molecules for the next stage in the preclinical development program. Out of all of the synthesized compounds submitted to NCI, 16 PQ analogues, namely, **PQ1** (NCI: D-826644/1), **PQ2** (NCI: D-826641/1), **PQ3** (NCI: D-826645/1), **PQ4** (NCI: D-826642/1), **PQ5** (NCI: D-826646/1), **PQ6** (NCI: D-826643/1), **ClPQ1** (NCI: D-826650/1), **ClPQ2** (NCI: D-826647/1), **ClPQ3** (NCI: D-826899/1), **ClPQ4** (NCI: D-826648/1), **ClPQ5** (NCI: D-826900/1), **ClPQ6** (NCI: D-826649/1), **BrPQ3** (NCI: D-825202/1), **BrPQ4** (NCI: D-825203/1), **BrPQ5** (NCI: D-825205/1), and **BrPQ6** (NCI: D-825206/1), were selected by the NCI *in vitro* disease-oriented human cells screening panel assay. Among the 16 analogues, four molecules (**ClPQ1**, **ClPQ2**, **ClPQ3**, and **ClPQ5**) exhibited prominent activity at a single dose, particularly against leukemia and breast cancer cells, especially in T47D and MDA-MB-468 cells.

https://doi.org/10.1021/acsomega.2c03428
ACS Omega 2022, 7, 30250−30264

Table 1. Antiproliferative Activity Data as per the Single-Dose Assay at 10 μM Concentration as Percent Cell Growth of the Selected Hybrid Molecules

	Growth Percentage of Cell Lines in NCI 60															
Molecule panel/Cancer Cell Line	PQ1	PQ2	PQ3	PQ4	PQ5	PQ6	ClPQ1	ClPQ2	ClPQ3	ClPQ4	ClPQ5	ClPQ6	BrPQ3	BrPQ4	BrPQ5	BrPQ6
Leukemia																
CCRF-CEM	52.77	71.22	108.04	54.38	78.84	76.30	6.54	9.06	13.93	88.98	21.91	107.17	97.74	87.25	8.53	72.07
HL-60(TB)	42.04	81.44	99.60	52.99	71.04	72.93	60.38	41.33	31.22	99.53	67.95	104.45	85.02	86.87	54.92	96.36
K-562	69.33	81.01	94.85	61.57	77.22	70.89	5.25	4.61	0.17	97.14	21.59	105.92	89.94	102.18	0.00	95.32
MOLT-4	40.03	57.18	101.32	41.29	64.96	67.50	11.32	9.07	5.67	104.91	45.34	109.10	95.53	91.31	12.51	97.78
RPMI-8226	80.82	85.81	110.82	66.08	75.80	70.05	58.31	36.54	26.75	107.63	10.30	112.89	ND	ND	ND	ND
SR	45.45	63.61	116.87	50.30	81.82	70.61	30.02	13.57	27.72	99.15	16.28	99.82	110.19	111.24	15.89	131.86
Non-Small-Cell Lung Cancer																
A549/ATCC	109.38	104.22	96.69	116.92	106.50	107.99	114.63	81.54	102.08	105.55	90.39	102.93	98.63	99.04	95.64	102.96
EKVX	100.21	100.07	92.95	94.60	81.16	71.09	92.15	53.20	74.38	103.49	90.24	104.62	97.50	97.43	102.76	97.15
HOP-62	97.37	70.92	104.54	70.52	78.37	93.63	94.81	66.19	103.34	100.98	103.15	95.29	98.48	91.51	92.56	93.81
HOP-92	123.17	117.32	110.93	113.05	78.75	100.71	33.94	64.89	54.21	97.27	56.40	105.82	95.48	88.13	−32.45	109.52
NCI-H226	94.96	94.65	102.24	95.58	64.46	85.98	85.86	72.88	100.11	95.85	91.34	102.69	92.31	93.04	86.48	94.44
NCI-H23	63.85	80.53	99.79	51.01	28.83	25.02	92.41	68.45	91.91	99.00	92.39	103.17	90.80	86.29	85.88	87.16
NCI-H322M	104.29	106.82	101.45	103.78	94.48	100.27	100.11	99.64	104.87	101.28	99.54	103.15	92.90	96.58	91.11	98.17
NCI-H460	104.08	100.07	102.51	98.38	93.08	96.39	100.81	79.33	101.27	103.41	99.81	102.79	102.63	101.23	99.65	104.73
NCI-H522	93.59	92.40	97.76	87.47	82.18	80.47	95.76	53.05	95.00	97.06	81.67	93.91	97.72	95.13	67.42	91.38
Colon Cancer																
COLO 205	114.22	99.59	114.73	114.90	106.70	116.33	113.94	103.57	122.07	110.59	117.91	107.65	114.36	113.00	113.64	119.97
HCC-2998	110.48	100.05	95.70	101.01	102.57	107.37	98.21	71.05	111.46	97.76	99.02	100.07	108.24	106.31	100.50	101.33
HCT-116	66.68	83.09	105.34	56.54	75.16	68.46	70.15	32.36	84.91	95.00	72.60	95.37	101.73	106.10	62.35	110.06
HCT-15	93.78	93.68	94.54	88.48	60.45	63.75	112.08	39.95	99.29	105.24	80.22	105.24	97.27	94.67	73.24	105.32
HT29	110.09	108.41	99.69	110.01	104.04	101.48	104.74	63.25	109.76	102.83	98.16	101.23	114.49	114.19	118.25	103.30
KM12	97.13	48.91	101.93	46.14	88.68	97.28	49.21	6.69	89.58	98.19	99.20	100.15	105.59	106.29	99.94	112.79
SW-620	103.88	100.94	102.71	101.24	94.81	98.14	102.58	35.52	100.22	103.09	88.67	102.02	101.08	101.15	91.34	107.30
CNS Cancer																
SF-268	97.34	88.87	99.81	85.57	80.45	86.97	97.45	87.28	92.83	98.80	92.02	96.69	97.25	99.03	93.68	97.28
SF-295	114.51	44.10	103.09	52.07	94.26	91.54	108.06	36.57	101.73	102.23	105.22	109.71	94.80	97.23	101.04	99.67
SF-539	97.20	102.06	99.64	99.16	89.94	100.02	99.35	65.91	95.82	100.81	96.63	100.53	98.49	91.68	94.74	102.54
SNB-19	96.18	72.52	94.01	71.94	78.17	86.38	86.95	53.53	96.47	96.73	91.50	91.08	98.72	93.89	84.56	96.73
SNB-75	93.39	86.61	88.26	78.75	70.97	73.68	60.67	64.48	104.24	71.33	58.44	75.21	87.16	72.84	59.68	81.68
U251	94.71	87.77	102.12	81.59	64.31	60.80	101.75	59.39	90.87	109.39	88.54	98.21	100.58	101.57	90.72	101.92
Melanoma																
LOX IMVI	60.96	79.57	97.86	45.96	47.29	42.59	69.01	24.66	91.94	97.99	62.62	102.79	98.64	87.57	34.94	96.80
MALME-3M	97.94	107.64	103.38	97.14	64.93	80.61	95.80	84.98	103.79	92.11	94.42	97.81	96.33	92.50	88.32	96.18
M14	107.51	94.76	100.94	89.71	88.35	94.91	92.30	45.80	100.04	101.36	83.30	97.64	97.23	91.22	95.09	96.42
MDA-MB-435	101.11	54.41	106.06	44.19	87.12	92.24	103.81	7.23	103.95	103.61	103.23	101.85	ND	ND	ND	ND
SK-MEL-2	101.28	100.48	101.85	96.08	82.36	84.69	97.96	69.06	104.26	104.96	95.78	107.23	110.66	109.02	105.91	110.80
SK-MEL-28	110.99	113.12	99.21	108.98	96.52	100.72	110.22	75.88	109.57	104.64	103.98	99.79	106.94	103.45	101.07	105.18
SK-MEL-5	96.35	95.55	100.60	91.60	31.34	80.90	95.56	44.58	100.01	100.45	98.09	100.16	99.48	98.79	96.00	99.95

https://doi.org/10.1021/acsomega.2c03428
ACS Omega 2022, 7, 30250−30264

Table 1. continued

Molecule panel/Cancer Cell Line	Growth Percentage of Cell Lines in NCI 60															
	PQ1	PQ2	PQ3	PQ4	PQ5	PQ6	ClPQ1	ClPQ2	ClPQ3	ClPQ4	ClPQ5	ClPQ6	BrPQ3	BrPQ4	BrPQ5	BrPQ6
UACC-257	86.90	94.24	99.26	84.05	62.55	76.58	107.74	79.51	93.27	106.09	91.40	101.38	93.93	101.27	87.25	103.23
UACC-62	96.18	81.28	96.20	74.11	65.58	74.16	85.52	5.89	94.67	93.47	93.42	92.97	91.58	88.65	79.24	93.84
Ovarian Cancer																
IGROV1	89.48	106.65	105.95	79.19	72.91	81.56	56.19	70.41	32.15	107.85	12.41	108.97	101.32	97.77	86.65	97.42
OVCAR-3	8.14	53.41	103.95	0.63	6.18	77.94	94.20	30.08	99.81	107.52	100.92	105.81	112.35	113.71	77.70	112.53
OVCAR-4	24.26	45.50	97.01	−62.99	34.87	42.80	−36.75	32.43	−4.17	97.14	80.21	100.85	98.04	81.60	88.81	98.47
OVCAR-5	109.26	106.57	104.50	103.77	98.35	94.37	100.76	90.90	105.02	104.86	106.30	106.35	98.34	102.07	99.94	97.51
OVCAR-8	87.91	93.26	102.90	83.75	82.19	88.77	99.45	77.88	98.78	108.15	92.94	104.45	104.24	98.25	92.40	96.93
NCI/ADR-RES	87.21	72.33	101.63	65.43	75.95	86.46	98.23	65.17	102.46	99.93	97.55	98.32	98.62	91.89	94.72	104.14
SK-OV-3	104.51	94.88	108.45	91.98	90.54	105.61	105.52	86.17	107.27	103.80	103.28	104.20	101.53	99.93	93.20	99.20
Renal Cancer																
786-0	101.24	97.80	102.99	105.95	89.87	108.03	103.77	84.92	105.37	96.10	96.48	89.15	96.30	97.16	96.22	95.76
A498	78.67	80.15	91.82	84.33	66.88	80.90	87.72	58.57	89.09	77.15	59.82	86.61	100.34	96.38	87.30	107.71
ACHN	99.99	104.71	107.11	89.87	86.38	85.48	103.52	63.22	105.72	105.75	79.57	106.12	102.66	99.64	87.46	99.76
CAKI-1	86.50	93.56	99.83	69.25	71.50	80.94	94.18	43.34	89.39	98.75	76.07	97.07	99.05	97.06	96.41	98.30
RXF 393	94.16	103.65	99.01	93.19	73.37	84.27	104.39	65.76	101.79	100.53	103.24	109.34	104.27	109.92	94.89	117.30
SN12C	93.34	95.47	96.82	93.83	61.34	80.77	92.60	80.24	94.82	91.11	84.14	94.31	101.47	90.46	85.69	96.74
TK-10	133.49	116.92	96.10	137.17	125.08	131.07	149.52	111.54	129.20	97.35	115.87	92.03	98.33	128.87	122.20	116.87
UO-31	94.47	97.26	97.19	73.90	66.35	70.63	89.42	65.14	96.71	95.00	86.46	97.46	87.47	82.95	71.56	79.96
Prostate Cancer																
PC-3	79.68	63.78	104.53	49.00	76.67	82.26	71.94	36.56	85.59	91.61	76.95	102.46	101.98	94.55	71.68	93.88
DU-145	107.66	112.33	107.76	108.70	69.91	89.87	110.44	85.27	103.59	110.92	103.03	109.95	104.22	104.88	109.31	108.34
Breast Cancer																
MCF7	71.25	85.19	89.88	62.67	45.98	47.04	81.95	35.95	84.66	91.74	46.32	97.37	94.08	89.61	27.12	87.49
MDA-MB-231/ATCC	76.38	91.46	102.22	75.17	66.17	86.97	36.47	68.89	28.05	98.40	48.94	105.00	93.68	88.55	−36.13	100.68
HS 578T	116.01	106.36	97.72	94.08	79.41	90.43	88.13	77.09	95.89	92.68	97.15	98.58	102.01	91.25	92.81	101.63
BT-549	101.00	99.41	96.01	91.14	82.63	97.33	96.22	77.48	130.61	99.27	105.92	96.62	110.91	99.91	92.89	108.00
T47D	64.40	71.26	91.24	43.19	65.00	69.12	−18.11	−25.87	−37.45	93.25	4.99	93.57	98.86	94.70	−0.52	100.62
MDA-MB-468	65.92	35.13	90.62	13.79	37.51	31.25	−62.02	−45.95	−20.59	93.45	−23.58	97.39	94.17	91.15	−53.99	89.55

https://doi.org/10.1021/acsomega.2c03428
ACS Omega 2022, 7, 30250−30264

2.2.2. In Vitro Antiproliferative Activity at One-Dose Concentration. The one-dose results of each tested PQ analogue from Table 1 were reported in the form of a mean graph of the cell growth percentage (GP). Their one-dose mean graphs are presented in the supplementary file as Figures SI 17−32. All PQ analogues either having a halogen or not on the quinone skeleton or an alkyl group of the ester group in different positions on the benzocaine skeleton were inactive against some of the cancer cell lines, such as non-small-cell lung cancer, colon cancer (except for **ClPQ2**), CNS cancer, melanoma (except for **ClPQ2**), renal cancer, and prostate cancer. Among all of the PQ analogues, the chlorinated PQ analogues (**ClPQ1-6**) displayed maximum sensitivity toward many cancer cell lines, in particular, leukemia cell lines, compared to the nonhalogenated (**PQ1-6**) and the brominated PQ analogues (**BrPQ3-6**). Looking specifically at the chlorinated PQ analogues (**ClPQ1-6**), **ClPQ1**, **ClPQ2**, and **ClPQ3** displayed considerable antiproliferative activity against CCRF-CEM, K-562, MOLT-4, and SR leukemia cell lines, as shown in Table 1. Less activity was observed against most cancer cell lines for the nonhalogenated (**PQ1-6**). Surprisingly, within brominated PQ analogues (**BrPQ3-6**), only one analogue displayed maximum sensitivity. The analogue **BrPQ5**, having a bromine atom within the quinone moiety, showed the best antiproliferative activity toward CCRF-CEM, K-562, MOLT-4, and SR leukemia cell lines with 91.47, 100.00, 87.49, and 84.11% inhibition in tumor cell growth, respectively. **PQ1** showed GI% values of 91.86 and 75.74 for some of the subpanel cell lines like ovarian cancer OVCAR-3 and OVCAR-4, respectively. In addition to **PQ1**, **PQ4** exhibited a GI% value above 85% for OVCAR-3 as well as the breast cancer cell line, MDA-MB-468. Another activity was observed against OVCAR-3 with 93.82% inhibition for **PQ5**. Among the chlorinated PQ analogues, **ClPQ2** was the most potent analogue with above 90% GI% values for colon cancer KM12, melanoma MDA-MB-435, and melanoma UACC-62. On the other hand, **ClPQ5** exhibited GI% values of around 90% ovarian cancer IGROV1 and breast cancer T47D. Especially, having substituents at the R2 position on the benzocaine skeleton caused increased antiproliferative activity in breast cancer and leukemia.

2.2.3. Structure−Activity Relationship (SAR) Study. Herein, based on the observed results of the antiproliferative activity of the tested hybrid molecules as Plastoquinone analogues containing both quinone and benzocaine moieties, the structure−activity relationship (SAR) can be summarized by indicating the change of both the halogen or hydrogen atom within the quinone moiety and the alkyl group of the ester group in different positions on the benzocaine skeleton that affects the antiproliferative activity. Table 1 reveals valuable data about the SAR showing a simple correlation between the cytotoxic activity and the change in the hydrogen/halogen atom within the quinone moiety. In addition to this, there is also a simple correlation between the cytotoxic activity and the alkyl group of the ester moiety, especially in comparison to leukemia cell lines. First, the high growth percentage (GP) values of the nonhalogenated (**PQ1-6**) and the brominated PQ analogues (**BrPQ3-6**) against the leukemia cell lines indicated that the chlorinated PQ analogues (**ClPQ1-6**) had more inhibition potency than the other PQ analogues (**PQ1-6** and **BrPQ3-6**). We then investigated the effect of the position of the alkyl group of the ester moiety. Concerning the chlorinated PQ analogues (**ClPQ1-6**), it was verified that the methyl ester group at the para position significantly increased the activity on leukemia cell lines, showing excellent inhibition. Replacement of the methyl group with the ethyl or *tert*-butyl group decreased the activity (**ClPQ2** > **ClPQ4** > **ClPQ6**). A preliminary SAR analysis displayed that the introduction of the chlorine atom into the quinone moiety enhanced the cytotoxicity against leukemia cell lines. Additionally, the introduction of a methyl group in the ester moiety in the meta position clearly boots the cytotoxicity.

2.2.4. Cytotoxicity and Cell Proliferation. According to the *in vitro* antiproliferative activity at five-dose concentration results, **BrPQ5**, **CIPQ1**, and **CIPQ3** were the most promising compounds with anticancer activity against breast cancer cells, especially in T47D and MDA-MB-468 cells. Also, in a recent study, we evaluated the anticancer activity of different plastoquinone analogues in different breast cancer cells and determined promising anticancer activity against MCF7 cells.[26] T47D and MCF7 cells are ER, PR-positive, and HER2-negative cell models for breast cancer.[27] Thus, T47D and MCF7 cell lines were used to evaluate the anticancer activity of quinone-benzocaine hybrid molecules in breast cancer.

The cytotoxic effects were compared to a well-known chemotherapeutic drug, doxorubicin HCl (DOXO). Human umbilical vein endothelial cells (HUVECs) were used as the noncancerous cell line to evaluate the selectivity of the compounds. The IC_{50} values, defined as the half-maximal inhibitory concentration of cell growth, are presented in Table 2. As can be seen in Figure 3, after 24 h of treatment, **BrPQ5**, **CIPQ1**, and **CIPQ3** showed dose-dependent cytotoxic activity for all of the cell lines. Compound **CIPQ1**, which contains the methyl ester group in the meta position, was the most active compound, and IC_{50} values for **CIPQ1** in T47D and MCF7 cells were found to be 2.35 μM ± 0.30 and 6.53 μM ± 0.71, respectively. According to our results, quinone-benzocaine hybrid molecules exhibited a higher cytotoxic activity in breast cancer cells than noncancerous HUVEC cells, and all tested compounds had an excellent selectivity index in T47D cells. **CIPQ1** exhibited more potent anticancer activity in T47D and MCF7 cells when compared with DOXO. The promising anticancer activity of **CIPQ1** against breast cancer cell lines encouraged us to study its effects at the cellular level.

To confirm this further, the antiproliferative effects of **CIPQ1** against T47D and MCF7 cells were assessed using a colony formation assay. The number of colony-forming cells

Table 2. IC_{50} (μM) Values of BrPQ5, CIPQ1, and CIPQ3 and the Positive Control DOXO in T47D and MCF7 Breast Cancer Cell Lines and the HUVEC Noncancerous Cell Line[a]

		T47D	MCF7	HUVEC
BrPQ5	IC_{50}	3.96 ± 0.44	20.16 ± 1.62	37.90 ± 6.12
	SI	9.57	1.88	
ClPQ1	IC_{50}	2.35 ± 0.30	6.53 ± 0.71	15.30 ± 2.73
	SI	6.52	2.34	
ClPQ3	IC_{50}	4.23 ± 0.45	19.85 ± 2.39	32.60 ± 6.50
	SI	7.71	1.64	
DOXO	IC_{50}	85.98 ± 16.76	16.10 ± 2.19	43.43 ± 7.41
	SI	0.51	2.70	

[a]The values are expressed as the mean ± SEM. Selectivity index [SI = IC_{50}(HUVEC)/IC_{50}(cancer cell line)] of **BrPQ5**, **CIPQ1**, **CIPQ3**, and **DOXO**.

https://doi.org/10.1021/acsomega.2c03428
ACS Omega 2022, 7, 30250−30264

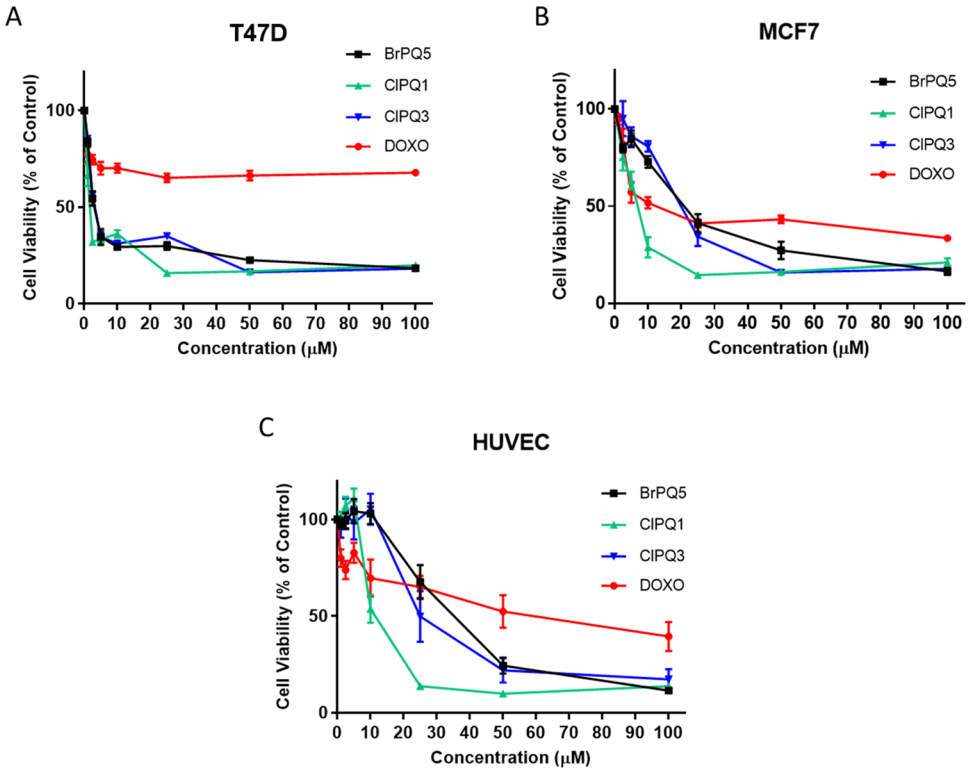

Figure 3. Cytotoxic effects of **BrPQ5**, **ClPQ1**, and **ClPQ3** on the growth of T47D (A) and MCF7 (B) breast cancer cell lines and the HUVEC (C) noncancerous cell line with the 3-(4,5-dimethylthiazol-2-yl)-2,5-diphenyltetrazolium bromide (MTT) assay for 24 h. The values are expressed as the mean ± SEM.

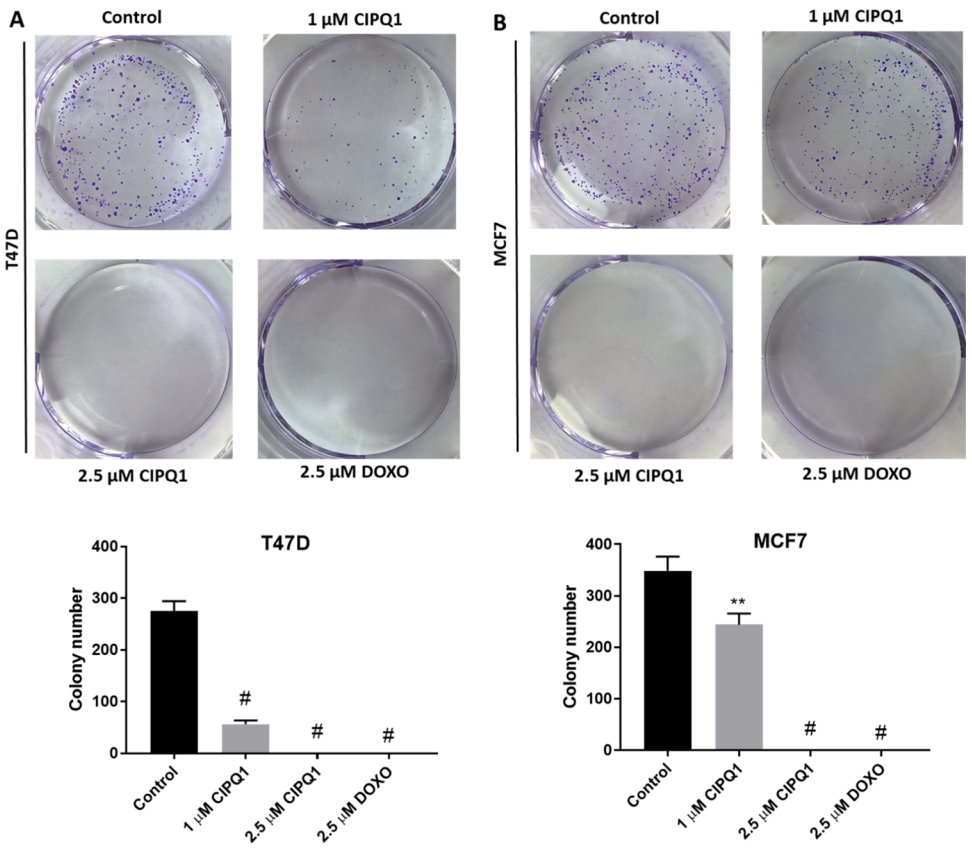

Figure 4. Antiproliferative effects of **ClPQ1** against T47D and MCF7 cells with the colony formation assay. Representative images and quantitative results of the colony formation assay with T47D (A) and MCF7 (B) cells. The values are expressed as mean ± SEM. $^{**}p < 0.01$; $^{\#}p < 0.0001$.

https://doi.org/10.1021/acsomega.2c03428
ACS Omega 2022, 7, 30250−30264

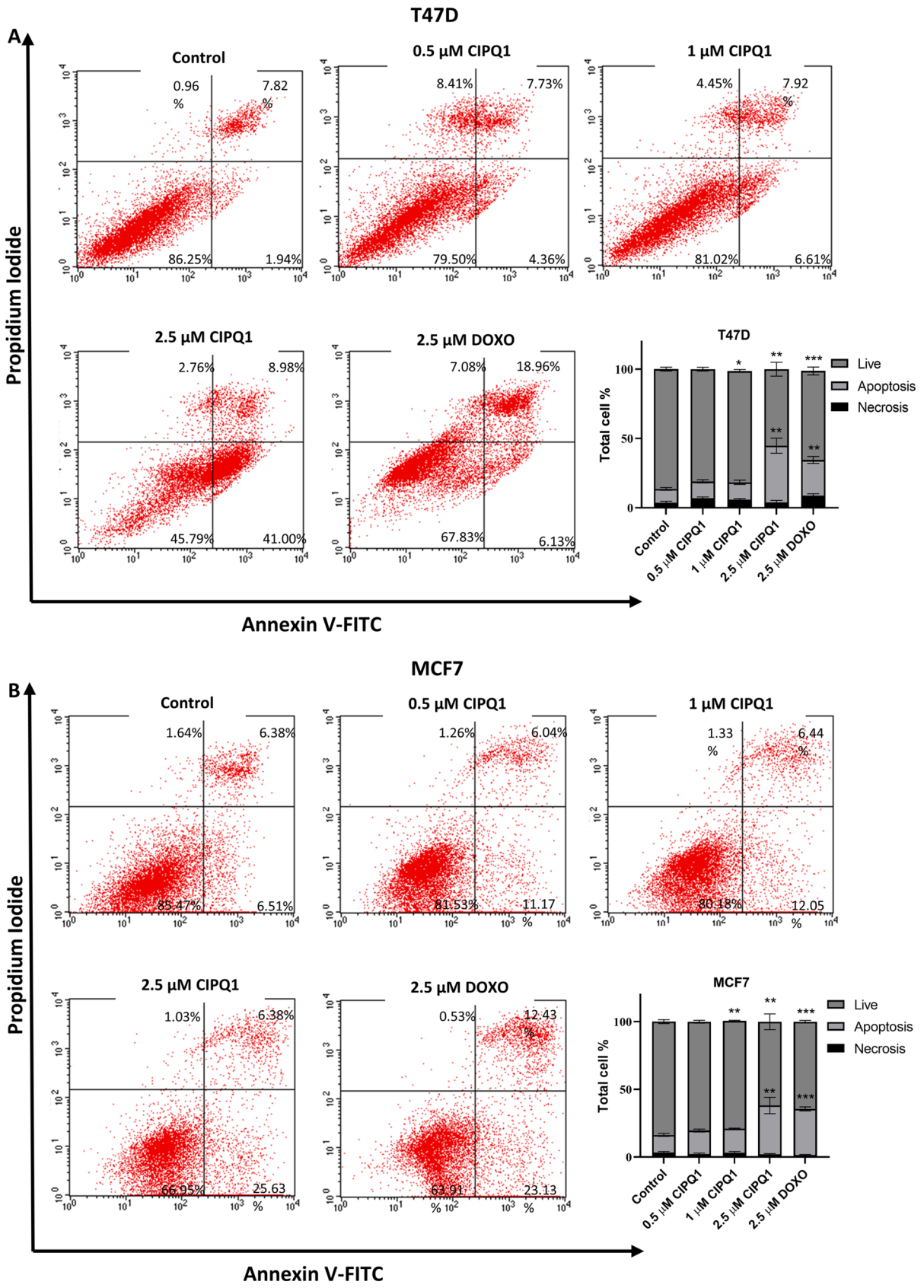

Figure 5. CIPQ1-induced apoptosis and necrosis were determined with Annexin V-FITC/PI double-staining by flow cytometry in T47D and MCF7 cells. Cells were classified as live cells (Annexin V^-, PI^-), apoptotic cells (Annexin V^+, PI^- and Annexin V^+, PI^+), and necrotic cells (Annexin V^-, PI^+). Representative images and the quantitative result of apoptosis analysis with T47D (A) and MCF7 (B) cells. The values are expressed as mean ± SEM. ***$p < 0.001$; $^{\#}p < 0.0001$.

https://doi.org/10.1021/acsomega.2c03428
ACS Omega 2022, 7, 30250−30264

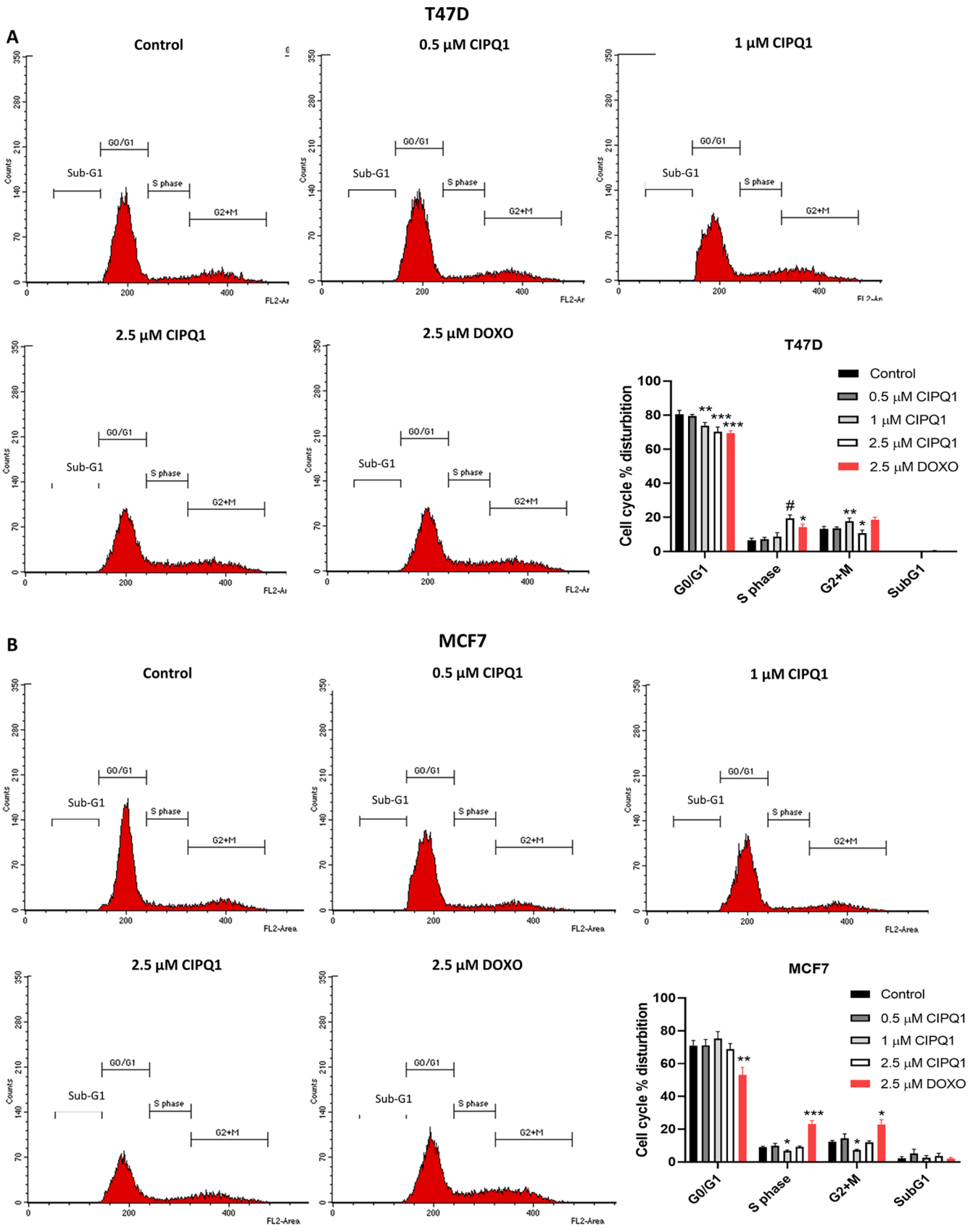

Figure 6. Effect of **CIPQ1** on the progression of T47D (A) and MCF7 (B) cell cycles as analyzed by flow cytometry. Representative cells cycle phase distribution histograms and the quantitative result of cell-cycle analysis. The values are expressed as the mean ± SEM. *$p < 0.05$, **$p < 0.01$, ***$p < 0.001$, $^{\#}p < 0.0001$.

https://doi.org/10.1021/acsomega.2c03428
ACS Omega 2022, 7, 30250−30264

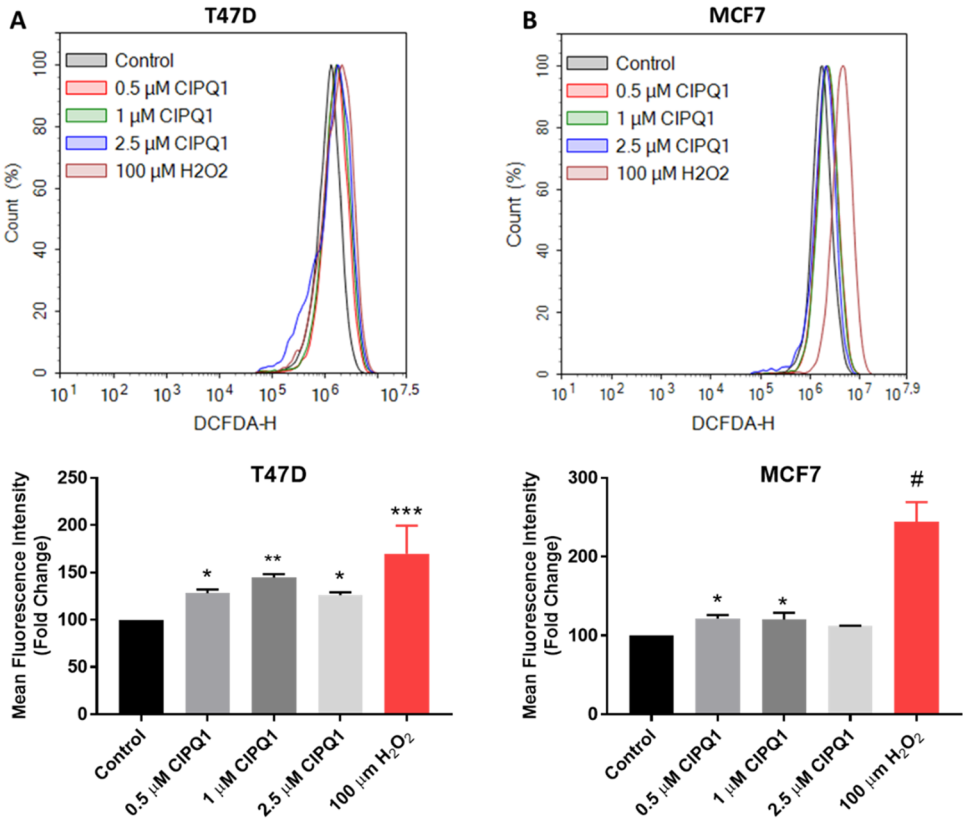

Figure 7. **CIPQ1**-induced oxidative stress was determined with DCDFA staining by flow cytometry in T47D (A) and MCF7 (B) cells. Representative DCDFA staining histograms and the quantitative result of ROS production analysis. The values are expressed as mean ± SEM. $^{*}p < 0.05$, $^{**}p < 0.01$, $^{***}p < 0.001$, and $^{\#}p < 0.0001$.

was reduced significantly at 1 μM concentration. The colonies disappeared entirely at 2.5 μM concentration for both cell lines, similar to the 2.5 μM DOXO group (Figure 4). Consistent with the MTT assay result, **CIPQ1** showed higher antiproliferative effects against T47D cells than MCF7 cells.

2.3.6. Detection of Apoptosis. Inhibition of cell proliferation and induction apoptosis in cancer cells with chemotherapeutic drugs has always been the focus of anticancer research.[28] To study the induction of apoptosis, T47D and MCF7 cells were treated with different concentrations of **CIPQ1** for 24 h. We analyzed by flow cytometry after double-staining with Annexin V-FITC and PI. Representative data and quantitative results from flow cytometry analyses are shown in Figure 5. A significant increase in the percentage of the apoptotic cells was observed in both T47D (41.01%) and MCF7 (36.17%) cells following 2.5 μM **CIPQ1** treatment in comparison to control groups (Figure 5). Apoptotic cells slightly increased following treatment with 0.5 μM and 1 μM concentrations of **CIPQ1** in both cell lines, but these changes were not significant compared to control data. Also, we used 2.5 μM DOXO as the positive control, and similar to **CIPQ1** treatment, a significant increase in the apoptosis rate was seen in the DOXO group for both cell lines.

In a similar study with chlorinated derivatives of 2-quinil-1,3-tropolones, Gusakov et al. reported that some of these compounds lead cells to apoptosis by affecting the ERK pathway, which is one of the pathways that ensure proliferation in colon (HCT-116) and ovarian cancers (OVCAR-3 and OVCAR-8).[29] In our earlier study on chlorinated plastoquinone analogues, we demonstrated for the first time the antiproliferative and apoptotic effects against K-562 cells. We also found that one analogue was as selective as imatinib, which is used in clinical practice.[11]

2.3.7. Cell-Cycle Evaluation. One of the important mechanisms of the cytotoxic action of many chemotherapeutic agents for the treatment of breast cancer is the arrest of the cell cycle at a specific checkpoint.[30] The effect of **CIPQ1** on cell-cycle distribution in T47D and MCF7 cells was determined by flow cytometry, and the cells showed alterations in the G0/G1, S, and G2 + M phases of the cell cycle under increased concentrations of **CIPQ1** (Figure 6). In T47D cells, 80.51% of the control cells were in the G0/G1 phase, 6.45% in the S phase, and 13.23% in the G2 + M phase. In MCF7 cells, 71.05% of the control cells were in the G0/G1 phase, 9.09% in the S phase, and 12.27% in the G2 + M phase. The number of G0/G1 (73.89%) cells in T47D cells was found to be significantly lower compared to the control group, and the cells in the G2 + M phase were significantly increased (17.69%) at 1 μM **CIPQ1** compared to the control group. In MCF7 cells at 1 μM **CIPQ1** concentration, the number of cells in the S phase (6.77%) and the G2 + M phase (7.29%) was found to be significantly low and the number of cells in the G0/G1 phase was higher, but no significant difference could be detected compared to the control group. Compared with the control, 2.5 μM **CIPQ1** reduced the cell percentage in the G2 + M and G0/G1 phases, while the percentage of cells increased in the S phase in T47D cells. However, 2.5 μM **CIPQ1** did not significantly induce G0/G1 cell accumulation in comparison to the control (68.78 versus 71.05%) in MCF7 cells. Compared to the control, a significant increase in G0/G1 arrest was

https://doi.org/10.1021/acsomega.2c03428
ACS Omega 2022, 7, 30250−30264

observed in both T47D and MCF7 cells treated with 2.5 μM DOXO treatment. The percentage of cells in G2 + M was similar to the 1 μM **CIPQ1** and 2.5 μM DOXO treatments in T47D cells. The effects of DOXO largely depend on drug concentration and treatment period *in vitro*.[31] Increased G2 + M arrest has been associated with enhanced apoptosis.[32] Thus, increased apoptosis with **CIPQ1** treatment may be related to G2 + M arrest in breast cancer cells.

2.3.8. Oxidative Stress. Increased intracellular reactive oxygen species (ROS) levels may lead to apoptosis induction and cell-cycle arrest. To further evaluate the toxicity mechanisms in the anticancer activity of **CIPQ1**, flow cytometric ROS level measurement was carried out by the 2′,7′-dichlorofluorescein-diacetate (DCDFA) probe after 24 h of **CIPQ1** treatment. As shown in Figure 7, **CIPQ1** significantly increased the ROS levels in all tested concentrations in T47D cells, while ROS increment was insignificant at the highest concentration in MCF7 cells. A 100 μM H_2O_2 treatment as a positive control for 30 min significantly increased the ROS level for both cell lines. ROS increment was more prominent in T47D cells than in MCF7 cells. Mild oxidative stress can activate the adaptive responses, and cells can maintain the cellular functions, whereas more severe oxidative stress can initiate apoptosis.[33] Thus, the increase of ROS at low concentrations of **CIPQ1** may induce changes to increase cell adaptation at high concentrations. ROS that exceeds the capacity of the cellular antioxidant system may lead T47D rather than MCF7 cells to apoptosis. Also, the higher cytotoxic and apoptotic activities of **CIPQ1** in T47D than in MCF7 cells may be related to the different levels of ROS induction.

2.3.9. Target Prediction and Molecular Docking. The "SwissTargetPrediction" server was employed to screen possible molecular target(s) of **CIPQ1**.[34] It showed the utmost probability to target both JNK1 and JNK3, which agrees with its antiproliferative effect. Intriguingly, **CIPQ1** demonstrated >0.9 3D structure similarity with three reported JNK pan inhibitors[35] as being output by the SwissSimilarity tool.[36] Therefore, **ClPQ1** has a great potential to be a JNK inhibitor, which may play a major in-part role in its antiproliferative mechanism.

We selected JNK3 cocrystallized with the compound **III** structure as a model to practically evaluate **CIPQ1** interaction with JNK3 and to verify our hypothesis. The binding free energy ΔG is −7.03 kcal/mol, implying the formation of a stable complex. **CIPQ1** is adopted effectively in the ATP binding site with a crucial H-bond with the gatekeeper Met146. Similar to **III**, **CIPQ1** quinone forms a H-bond with Met149 in the backbone hinge region. The terminal phenyl benzoate is implicated in van der Waals contacts with Leu206 and Lys93 (Figure 8). Noticeably, an intramolecular non-standard H-bond between C═O of the quinone benzoate moiety is observed; such a type of interaction efficiently stabilizes the formed complex. Conclusively, **CIPQ1** has a considerable affinity to JNK3, comparable to the cocrystallized ligand **III**.

2.3.10. In Silico Drug-Likeness and ADME Analysis of CIPQ1. Drug-likeness and ADME prediction of new chemical entities are significant in modern medicinal chemistry. The SwissADME server, a free tool for drug-likeness prediction, was applied for calculating several molecular and structural features of **CIPQ1**. It can be easily transported in the body due to its small molecular weight (319.74 g/mol). This small molecular

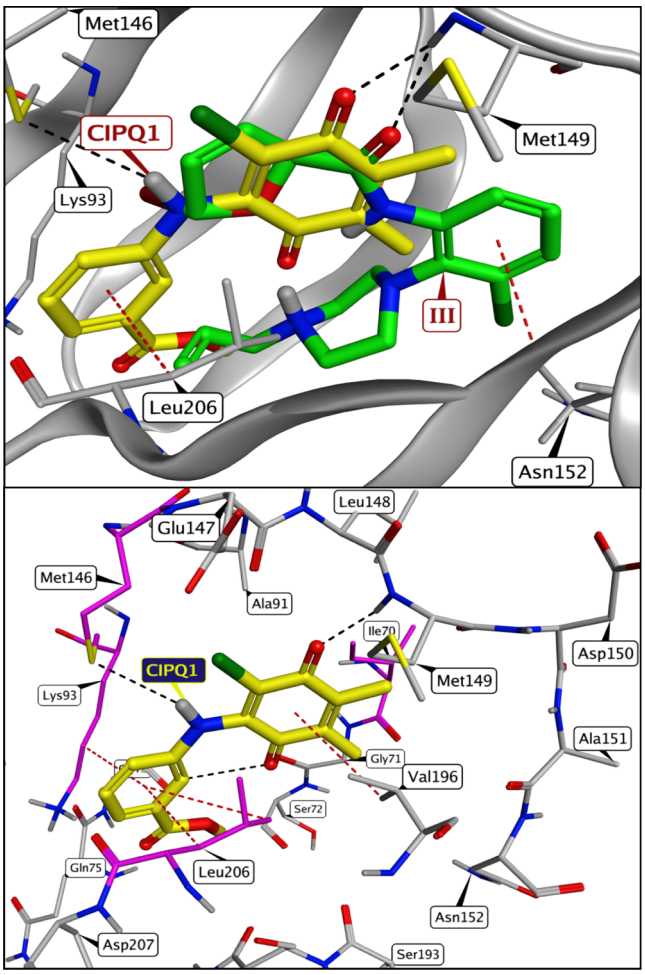

Figure 8. Overlaid **CIPQ1** (yellow) and III (green) in JNK3 ATP binding sites followed by a detailed binding mode of **CIPQ1** showing H-bonds with Met146 and Met149, intramolecular H-bonds (black-dashed lines), and van der Waals contacts (red-dashed lines).

weight makes it an ideal lead compound that can be chemically modified to enhance its potency. Its octanol−water partition coefficient (log P), which indicates lipophilicity, is 2.7, i.e., in the acceptable range (−0.4 to 5.6). Its total polar surface area is TPSA 72.47 Å^2. Furthermore, the number of hydrogen-bond acceptors (HBAs < 4) and the number of hydrogen-bond donors (HBDs < 1) are in the acceptable ranges. However, it is moderately soluble. Taken together, **CIPQ1** is assumed to have good oral bioavailability.

SwissADME calculations revealed that the titled compound possesses lead-likeness properties[37] and they obey all Lipinski,[38] Ghose,[39] Veber,[40] Egan,[41] and Muegge[42] rules for drug-likeness without any violations. It is noteworthy to mention the appearance of some alerts regarding possible interference with some CYP450 isoforms.

3. CONCLUSIONS

With the rapidly growing field of drug design and discovery, the determination and identification of important pharmacophoric moieties by a large amount of research and molecular hybridization is of great interest. Herein, we combined two important pharmacophoric moieties, i.e., benzocaine analogues and 2,3-dimethlylquinone, and identified an active scaffold against leukemia cancer cell lines in our laboratory.[11,12] To

https://doi.org/10.1021/acsomega.2c03428
ACS Omega 2022, 7, 30250−30264

summarize, three different series of quinone-benzocaine hybrid molecules as nonhalogenated and halogenated (brominated and chlorinated) PQ analogues were resynthesized, and 16 of 18 hybrid molecules were tested by NCI for their *in vitro* antiproliferative potential against the full NCI 60 cell line panel. The *in vitro* preliminary antiproliferative evaluation clearly showed that combining these two moieties could be a beneficial way to enhance the antiproliferative activity, particularly in leukemia cancer cell lines. According to the generation of the 18 hybrid molecules, they are basically divided into three series (nonhalogenated PQ analogues, brominated PQ analogues, and chlorinated PQ analogues). It was revealed that the nonhalogenated and brominated PQ analogues exhibited the poorest effects on cell growth at 10 μM concentration. The hybrid molecule **ClPQ2** showed distinguished antiproliferative activity against leukemia cancer cell lines in the five-dose concentration of NCI. As per the results obtained from *in vitro* antiproliferative evaluation, the hybrid molecule **ClPQ2** was identified as the most potent PQ analogue with the highest 50% growth inhibitory activity against the CCRF-CEM cell line of leukemia (1.08 GI_{50}), the SR cell line of leukemia (1.22 GI_{50}), and the DU-145 cell line of breast cancer (1.12 GI_{50}).

Subsequent testing was undertaken to determine the biological activity of **CIPQ1**, which exhibits the broadest activities against breast cancer cell lines of the quinone-benzocaine hybrid molecules. **ClPQ1** showed prominent antiproliferative effects in MCF7 and T47D cells from luminal type A breast cancers. Furthermore, **ClPQ1** dose-dependently reduced colony formation and induced apoptosis and ROS production in both cell lines. Apoptotic and cell-cycling effects were significant only at the highest concentration in MCF7 and T47D cells. **CIPQ1** demonstrated a strong *in silico* binding interaction with JNK3 comparable to the cocrystallized ligand compound **III** in addition to drug-likeness properties. Taken together, our study suggests that **ClPQ1** belongs to a promising new class of heterocyclic compounds that should be used for the future development of effective anticancer agents, especially in breast cancer.

4. EXPERIMENTAL SECTION

4.1. Biological Evaluation. *4.1.1. In Vitro Antiproliferative Activity at One-Dose Concentration by NCI.* Three different series of 2,3-dimethylquinone-benzocaine hybrid molecules as nonhalogenated and halogenated (brominated and chlorinated) PQ analogues were submitted to the National Cancer Institute (NCI), Bethesda, and as per the standard protocol of NCI, all compounds were evaluated for their antiproliferative activity at a single-dose assay (10 μM concentration in DMSO) on a panel of 60 cancer cell lines derived from leukemia, non-small-cell lung, colon, CNS, melanoma, ovarian, renal, prostate, and breast as per protocol. Tested compounds were added to microtiter culture plates, followed by incubation for 48 h at 37 °C. Sulforhodamine B (SRB), a protein-binding dye, was used for end-point determination. The percentage of the treated cells' growth was determined compared to the untreated control cells, and the results of each tested compound were reported. Data from one-dose experiments pertain to the percentage growth at 10 μM.[25,43]

4.1.2. In Vitro Antiproliferative Activity at Five-Dose Concentration by ***NCI.*** Serial 5 × 10-fold dilution from an initial DMSO stock solution was performed prior to incubation at each individual concentration. The most promising chlorinated PQ analogue (**ClPQ2**) was then elevated by DTP-NCI for a higher testing level to determine three dose−response parameters (GI_{50}, TGI, and LC_{50}) for each cell line after establishing a dose−response curve from five different concentrations of 0.01, 0.1, 1, 10, and 100 μM for **ClPQ2**. The exact detailed procedure for the latter assay had been elaborated earlier.[43,44]

4.2. *In Silico* Study. *4.2.1. Molecular Docking.* The "SwissTargetPrediction" server was employed to screen possible molecular target(s) of **CIPQ1**.[34] JNK3 cocrystallized with compound **III** was retrieved from the Protein Data Bank to be utilized as a model in the present study (PDB: 3FV8). The protein structure was prepared using the QuickPrep module of MOE (Version 2019.01, Chemical Computing Group Inc., Montreal, QCstate abbrev, Canada). The docking study was conducted using the rigid-receptor method.[45] The cocrystallized ligand **III** was defined as the center of the binding site. Using the MOE build suite, the chemical structures were drawn and energy-minimized using the MOE default force field.[46] All other docking parameters were kept at their default values. Fifteen docking positions for **CIPQ1** were generated. The generated docking positions were visualized using MOE.

4.7. *In Silico* Drug-Likeness and ADMET Analysis. The online SwissADME server was employed to predict the drug-likeness and ADME parameters.[47]

4.3. Cell Culture Experiment. *4.3.1. Cell Culture and Cytotoxicity Assay.* MCF7 cells were maintained in DMEM:F12, T47D cells were maintained in RPMI, and HUVEC cells were maintained in DMEM. The mediums were supplemented with heat-inactivated 10% FBS and penicillin-streptomycin (100 U/mL and 100 mg/mL) in a humidified incubator with 5% CO_2 at 37 °C.

The cytotoxic potential of the compounds was investigated with an MTT assay. Briefly, a total of 1.5×10^4 cells per well were seeded in 96-well plates and incubated overnight. Then, the medium was discarded, and the cells were treated with concentrations of each compound (1−100 μM) dissolved in DMSO. Control cells received 0.5% DMSO, the final DMSO concentration for compound treatments. After 24 h, the MTT solution was added to the wells (5 mg/mL) and further incubated for 3 h. Then, formazan precipitate was dissolved in DMSO, and the absorbance values were read at 590 nm with a microplate reader (Biotek). The concentration resulting in a 50% inhibition (IC_{50} value) was calculated from the dose−response curve.

4.3.2. Colony Formation Assay. For the colony formation assay, T47D and MCF7 cells were seeded at a density of 1000 cells per well in 6-well plates and left overnight. Then, the cells were treated with 1 μM and 2.5 μM **CIPQ1** and 2.5 μM DOXO as a positive control for 24 h. Next, 0.5% DMSO-treated cells were used as negative controls. Post incubation, the medium was discarded, and the cells were incubated in a fresh medium to form colonies for a period of 10 days. After 10 days, the wells were washed with PBS, and the cells were fixed with cold methanol for 5 min and stained with 0.5% crystal violet for 20 min. Then, the excess dye was washed with distilled water, and the plates were air-dried. The results of colony formations were photographed under natural light, and the colonies were counted using Vilber Lourmat Quantum Software (Vilber Lourmat).

https://doi.org/10.1021/acsomega.2c03428
ACS Omega 2022, 7, 30250−30264

4.3.3. Oxidative Stress. The intracellular ROS levels were measured with 2′,7′-dichlorofluorescein-diacetate (DCFDA) by flow cytometry. T47D and MCF7 cells were seeded at a density of 4×10^5 cells per well in 6-well plates and left overnight. Then, the cells were treated with 0.5 μM, 1 μM, and 2.5 μM **CIPQ1** for 24 h; 100 μM H_2O_2-treated cells (for 30 min) were used as positive controls, and 0.5% DMSO-treated cells were used as negative controls. After treatments, cells were collected by trypsinization and stained with 20 μM DCDFA for 15 min. Then, the fluorescent value for each group was determined with flow cytometry NovoCyte (Agilent) analyzed by using NovoExpress (Agilent) software.

4.3.4. Detection of Apoptosis. According to the manufacturer's protocol, the apoptotic and necrotic cell rates were analyzed with Annexin V-FITC and PI (Sony) staining. For the assay, the MCF7 and T47D cells were treated with 0.5 μM, 1 μM, and 2.5 μM **CIPQ1** and 2.5 μM DOXO along with the control for 24 h. Then, the cells were collected by trypsinization and centrifuged at 300*g* for 10 min. The cells were stained with Annexin V-FITC and PI and incubated for 15 min at room temperature. The flow cytometric analysis was carried out immediately afterward by FACS Calibur flow cytometry (BD Bioscience). The percentages of apoptotic and necrotic cells were calculated using BD Bioscience software (BD Bioscience).

4.3.5. Cell-Cycle Evaluation. The effect of **CIPQ1** on cell-cycle arrest was evaluated by the Muse Cell Cycle Kit (Millipore) according to the manufacturer's protocol. For the assay, the MCF7 and T47D cells were treated with 0.5 μM, 1 μM, and 2.5 μM **CIPQ1** and 2.5 μM DOXO along with the control for 24 h. The cells were collected by trypsinization and fixed in ice-cold 70% ethanol for 3 h. Subsequently, the cells were collected by 300*g* centrifugation for 5 min. The cell pellet was suspended in a 200 μL assay buffer and incubated for 30 min in the dark. The differences in the cell-cycle stages (G0/G1, S, G2 + M, sub-G1) were analyzed by FACS Calibur flow cytometry (BD Biosciences) and calculated using BD Bioscience software.

4.3.6. Statistical Analysis. GraphPad 7 software was used to evaluate the data. All experiments were performed at least in triplicate. Data are reposted as the mean standard error (SEM). The mean values of groups were compared with one-way ANOVA with Dunnett's multiple-comparison test. *P*-value < 0.05 was considered statistically significant.

4.3.7. Materials. DMEM:F12, RPMI, and DMEM mediums, heat-inactivated FBS, penicillin-streptomycin, and PBS were from Gibco. MCF7, T47D, and HUVEC cells were obtained from ATCC. 2′,7′-Dichlorofluorescein-diacetate, crystal violet, and ethanol were bought from Sigma. The Muse Cell Cycle Kit was from Millipore. Annexin V-FITC and PI kits were from Sony. Doxorubicin HCl was from Saba. DMSO was purchased from Bioshop Canada. MTT and trypsin were from BioMatik.

■ ASSOCIATED CONTENT

Supporting Information

The Supporting Information is available free of charge at https://pubs.acs.org/doi/10.1021/acsomega.2c03428.

Purity chromatograms of the hybrid molecules (**PQ1-6**, **BrPQ1-6**, and **ClPQ1-6**) and single-dose *in vitro* antiproliferative activity data (**PQ1-6**, **BrPQ1-6**, and **ClPQ1-6**) (PDF)

■ AUTHOR INFORMATION

Corresponding Author

Amaç Fatih TuYuN − *Department of Chemistry, Faculty of Science, Istanbul University, 34126 Istanbul, Turkey;* orcid.org/0000-0001-5698-1109; Phone: +90212 440 0000; Email: aftuyun@gmail.com, aftuyun@istanbul.edu.tr

Authors

Ayse Mine Yilmaz Goler − *Department of Biochemistry, School of Medicine/Genetic and Metabolic Diseases Research and Investigation Center, Marmara University, 34854 Istanbul, Turkey*

Ayse Tarbin Jannuzzi − *Department of Pharmaceutical Toxicology, Faculty of Pharmacy, Istanbul University, 34126 Istanbul, Turkey*

Nilüfer Bayrak − *Department of Chemistry, Faculty of Engineering, Istanbul University-Cerrahpasa, 34320 Istanbul, Turkey*

Mahmut Yıldız − *Department of Chemistry, Gebze Technical University, Gebze 41400 Kocaeli, Turkey;* orcid.org/0000-0001-6317-5738

Hatice Yıldırım − *Department of Chemistry, Faculty of Engineering, Istanbul University-Cerrahpasa, 34320 Istanbul, Turkey*

Masami Otsuka − *Medicinal and Biological Chemistry Science Farm Joint Research Laboratory, Faculty of Life Sciences, Kumamoto University, Kumamoto, Kumamoto 862-0973, Japan; Department of Drug Discovery, Science Farm Ltd., Kumamoto, Kumamoto 862-0976, Japan;* orcid.org/0000-0002-2968-3939

Mikako Fujita − *Medicinal and Biological Chemistry Science Farm Joint Research Laboratory, Faculty of Life Sciences, Kumamoto University, Kumamoto, Kumamoto 862-0973, Japan*

Mohamed O. Radwan − *Medicinal and Biological Chemistry Science Farm Joint Research Laboratory, Faculty of Life Sciences, Kumamoto University, Kumamoto, Kumamoto 862-0973, Japan; Chemistry of Natural Compounds Department, Pharmaceutical and Drug Industries Research Division, National Research Centre, Dokki, Cairo 12622, Egypt*

Complete contact information is available at: https://pubs.acs.org/10.1021/acsomega.2c03428

Author Contributions

◆A.M.Y.G. and A.T.J. contributed equally to this work.

Notes

The authors declare no competing financial interest.

■ ACKNOWLEDGMENTS

This work was financially supported by the Scientific Research Projects Coordination Unit of Istanbul University-Cerrahpasa (Project numbers: FBA-2018-29424) by supplying the equipment and materials.

■ REFERENCES

(1) Bolognesi, M. L.; Calonghi, N.; Mangano, C.; Masotti, L.; Melchiorre, C. Parallel synthesis and cytotoxicity evaluation of a polyamine-quinone conjugates library. *J. Med. Chem.* **2008**, *51*, 5463−5467.

(2) Li, Y.-R.; Liu, F.-F.; Liu, W.-B.; Zhang, Y.-F.; Tian, X.-Y.; Fu, X.-J.; Xu, Y.; Song, J.; Zhang, S.-Y. A novel aromatic amide derivative SY-65 co-targeted tubulin and histone deacetylase 1 with potent

anticancer activity in vitro and in vivo. *Biochem. Pharmacol.* **2022**, *201*, No. 115070.
(3) Ji, H. F.; Li, X. J.; Zhang, H. Y. Natural products and drug discovery Can thousands of years of ancient medical knowledge lead us to new and powerful drug combinations in the fight against cancer and dementia? *Embo. Rep.* **2009**, *10*, 194−200.
(4) (a) Sun, Y.-X.; Song, J.; Kong, L.-J.; Sha, B.-B.; Tian, X.-Y.; Liu, X.-J.; Hu, T.; Chen, P.; Zhang, S.-Y. Design, synthesis and evaluation of novel bis-substituted aromatic amide dithiocarbamate derivatives as colchicine site tubulin polymerization inhibitors with potent anticancer activities. *Eur. J. Med. Chem.* **2022**, *229*, 114069. (b) Song, J.; Guan, Y.-F.; Liu, W.-B.; Song, C.-H.; Tian, X.-Y.; Zhu, T.; Fu, X.-J.; Qi, Y.-Q.; Zhang, S.-Y. Discovery of novel coumarin-indole derivatives as tubulin polymerization inhibitors with potent anti-gastric cancer activities. *Eur. J. Med. Chem.* **2022**, *238*, 114467.
(5) Bentley, R. Different roads to discovery; Prontosil (hence sulfa drugs) and penicillin (hence beta-lactams). *J. Ind. Microbiol. Biotechnol.* **2009**, *36*, 775−786.
(6) Durand, G. A.; Raoult, D.; Dubourg, G. Antibiotic discovery: history, methods and perspectives. *Int. J. Antimicrob. Agents* **2019**, *53*, 371−382.
(7) Ferlay, J.; Ervik, M.; Lam, F.; Colombet, M.; Mery, L.; Piñeros, M.; Znaor, A.; Soerjomataram, I.; Bray, F. *Global Cancer Observatory: Cancer Today*; International Agency for Research on Cancer: Lyon, France, 2020. Available from: https://gco.iarc.fr/today (accessed Feb 19, 2021).
(8) Crawford, J. M.; Tang, G. L.; Herzon, S. B. Natural Products: An Era of Discovery in Organic Chemistry. *J. Org. Chem.* **2021**, *86*, 10943−10945.
(9) (a) Gatadi, S.; Gour, J.; Nanduri, S. Natural product derived promising anti-MRSA drug leads: A review. *Bioorg. Med. Chem.* **2019**, *27*, 3760−3774. (b) Sharifi-Rad, J.; Ozleyen, A.; Boyunegmez Tumer, T.; Tumer, T. B.; Oluwaseun Adetunji, C.; Adetunji, C. O.; El Omari, N.; Balahbib, A.; Taheri, Y.; Bouyahya, A.; Martorell, M.; Martins, N. Natural Products and Synthetic Analogs as a Source of Antitumor Drugs. *Biomolecules* **2019**, *9*, No. 679. (c) Taverna, S.; Corrado, C. Natural Compounds: Molecular Weapons against Leukemia's. *J. Leuk.* **2017**, *05*, 2.
(10) (a) Lodygin, D.; Menssen, A.; Hermeking, H. Induction of the Cdk inhibitor p21 by LY83583 inhibits tumor cell proliferation in a p53-independent manner. *J. Clin. Invest.* **2002**, *110*, 1717−1727. (b) Tandon, V. K.; Chhor, R. B.; Singh, R. V.; Rai, S. J.; Yadav, D. B. Design, synthesis and evaluation of novel 1,4-naphthoquinone derivatives as antifungal and anticancer agents. *Bioorg. Med. Chem. Lett.* **2004**, *14*, 1079−1083. (c) Keinan, S.; Paquette, W. D.; Skoko, J. J.; Beratan, D. N.; Yang, W.; Shinde, S.; Johnston, P. A.; Lazo, J. S.; Wipf, P. Computational design, synthesis and biological evaluation of para-quinone-based inhibitors for redox regulation of the dual-specificity phosphatase Cdc25B. *Org. Biomol. Chem.* **2008**, *6*, 3256−3263.
(11) Bayrak, N.; Yildirim, H.; Yildiz, M.; Radwan, M. O.; Otsuka, M.; Fujita, M.; Ciftci, H. I.; Tuyun, A. F. A novel series of chlorinated plastoquinone analogs: Design, synthesis, and evaluation of anticancer activity. *Chem. Biol. Drug Des.* **2020**, *95*, 343−354.
(12) (a) Bayrak, N.; Yildirim, H.; Yildiz, M.; Radwan, M. O.; Otsuka, M.; Fujita, M.; Tuyun, A. F.; Ciftci, H. I. Design, synthesis, and biological activity of Plastoquinone analogs as a new class of anticancer agents. *Bioorg. Chem.* **2019**, *92*, No. 103255. (b) Ciftci, H. I.; Bayrak, N.; Yildirim, H.; Yildiz, M.; Radwan, M. O.; Otsuka, M.; Fujita, M.; Tuyun, A. F. Discovery and structure-activity relationship of plastoquinone analogs as anticancer agents against chronic myelogenous leukemia cells. *Arch. Pharm.* **2019**, *352*, No. e1900170.
(13) (a) Bayrak, N.; Ciftci, H. I.; Yildiz, M.; Yildirim, H.; Sever, B.; Tateishi, H.; Otsuka, M.; Fujita, M.; Tuyun, A. F. Structure based design, synthesis, and evaluation of anti-CML activity of the quinolinequinones as LY83583 analogs. *Chem. Biol. Interact.* **2021**, *345*, No. 109555. (b) Ciftci, H. I.; Bayrak, N.; Yıldız, M.; Yıldırım, H.; Sever, B.; Tateishi, H.; Otsuka, M.; Fujita, M.; Tuyun, A. F. Design, synthesis and investigation of the mechanism of action underlying anti-leukemic effects of the quinolinequinones as LY83583 analogs. *Bioorg. Chem.* **2021**, *114*, No. 105160.
(14) (a) Khair-ul-Bariyah, S.; Arshad, M.; Ali, M.; Din, M. I.; Sharif, A.; Ahmed, E. Benzocaine: Review on a Drug with Unfold Potential. *Mini-Rev. Med. Chem.* **2020**, *20*, 3−11. (b) Ram, P. S.; Saraswathy, T.; Niraimathi, V.; Indhumathi, B. Synthesis, characterization and antimicrobial activity of some hetero benzocaine derivatives. *Int. J. Pharm. Pharm. Sci.* **2012**, *4*, 285−287. (c) Zhakina, A. K.; Kurapova, M. Y.; Gazaliev, A. M.; Nurkenov, O. A. Synthesis and biological activity of certain derivatives of anesthesine (benzocaine). *Russ. J. Gen. Chem.* **2008**, *78*, 1253−1254.
(15) (a) Lal, K.; Yadav, P.; Kumar, A.; Kumar, A.; Paul, A. K. Design, synthesis, characterization, antimicrobial evaluation and molecular modeling studies of some dehydroacetic acid-chalcone-1,2,3-triazole hybrids. *Bioorg. Chem.* **2018**, *77*, 236−244. (b) Venepally, V.; Jala, R. C. R. An insight into the biological activities of heterocyclic-fatty acid hybrid molecules. *Eur. J. Med. Chem.* **2017**, *141*, 113−137.
(16) Zhou, J.; Duan, L.; Chen, H. M.; Ren, X. M.; Zhang, Z.; Zhou, F. T.; Liu, J. S.; Pei, D. Q.; Ding, K. Atovaquone derivatives as potent cytotoxic and apoptosis inducing agents. *Bioorg. Med. Chem. Lett.* **2009**, *19*, 5091−5094.
(17) Bayrak, N.; Yildiz, M.; Yildirim, H.; Mataraci-Kara, E.; Tuyun, A. F. Novel plastoquinone analogs containing benzocaine and its analogs: structure-based design, synthesis, and structural characterization. *Res. Chem. Intermed.* **2021**, *47*, 2125−2141.
(18) (a) Perou, C. M.; Sørlie, T.; Eisen, M. B.; van de Rijn, M.; Jeffrey, S. S.; Rees, C. A.; Pollack, J. R.; Ross, D. T.; Johnsen, H.; Akslen, L. A.; et al. Molecular portraits of human breast tumours. *Nature* **2000**, *406*, 747−752. (b) Sørlie, T.; Perou, C. M.; Tibshirani, R.; Aas, T.; Geisler, S.; Johnsen, H.; Hastie, T.; Eisen, M. B.; van de Rijn, M.; Jeffrey, S. S.; et al. Gene expression patterns of breast carcinomas distinguish tumor subclasses with clinical implications. *Proc. Natl. Acad. Sci. U.S.A.* **2001**, *98*, 10869−10874.
(19) (a) Kondov, B.; Milenkovikj, Z.; Kondov, G.; Petrushevska, G.; Basheska, N.; Bogdanovska-Todorovska, M.; Tolevska, N.; Ivkovski, L. Presentation of the Molecular Subtypes of Breast Cancer Detected By Immunohistochemistry in Surgically Treated Patients. *Open Access Maced. J. Med. Sci.* **2018**, *6*, 961−967. (b) Sledge, G. W.; Mamounas, E. P.; Hortobagyi, G. N.; Burstein, H. J.; Goodwin, P. J.; Wolff, A. C. Past, present, and future challenges in breast cancer treatment. *J. Clin. Oncol.* **2014**, *32*, 1979−1986.
(20) Fulda, S.; Galluzzi, L.; Kroemer, G. Targeting mitochondria for cancer therapy. *Nat. Rev. Drug Discovery* **2010**, *9*, 447−464.
(21) (a) Hassan, A. N.; Toma, T.; Ciftci, H.; Biswas, T.; Tahara, Y.; Radwan, M. O.; Tateishi, H.; Fujita, M.; Otsuka, M. A vitamin D C/D ring-derived compound with cytotoxicity. *Med. Chem. Res.* **2022**, *31*, 1120−1125. (b) Nishimura, N.; Radwan, M. O.; Amano, M.; Endo, S.; Fujii, E.; Hayashi, H.; Ueno, S.; Ueno, N.; Tatetsu, H.; Hata, H.; et al. Novel p97/VCP inhibitor induces endoplasmic reticulum stress and apoptosis in both bortezomib-sensitive and -resistant multiple myeloma cells. *Cancer Sci* **2019**, *110*, 3275−3287.
(22) Olson, J. M.; Hallahan, A. R. p38 MAP kinase: a convergence point in cancer therapy. *Trends Mol. Med.* **2004**, *10*, 125−129.
(23) Koch, P.; Gehringer, M.; Laufer, S. A. Inhibitors of c-Jun N-Terminal Kinases: An Update. *J. Med. Chem.* **2015**, *58*, 72−95.
(24) (a) Li, G.; Qi, W.; Li, X.; Zhao, J.; Luo, M.; Chen, J. Recent Advances in c-Jun N-Terminal Kinase (JNK) Inhibitors. *Curr. Med. Chem.* **2021**, *28*, 607−627. (b) Kumar, A.; Singh, U. K.; Kini, S. G.; Garg, V.; Agrawal, S.; Tomar, P. K.; Pathak, P.; Chaudhary, A.; Gupta, P.; Malik, A. JNK pathway signaling: a novel and smarter therapeutic targets for various biological diseases. *Future Med. Chem.* **2015**, *7*, 2065−2086. (c) Stebbins, J. L.; De, S. K.; Machleidt, T.; Becattini, B.; Vazquez, J.; Kuntzen, C.; Chen, L. H.; Cellitti, J. F.; Riel-Mehan, M.; Emdadi, A.; et al. Identification of a new JNK inhibitor targeting the JNK-JIP interaction site. *Proc. Natl. Acad. Sci. U.S.A.* **2008**, *105*, 16809−16813. (d) Yao, G.-D.; Ge, M.-Y.; Li, D.-Q.; Chen, L.; Hayashi, T.; Tashiro, S.-i.; Onodera, S.; Guo, C.; Song, S.-J.; Ikejima, T. L-A03, a dihydroartemisinin derivative, promotes apoptotic cell

https://doi.org/10.1021/acsomega.2c03428
ACS Omega 2022, 7, 30250−30264

death of human breast cancer MCF-7 cells by targeting c-Jun N-terminal kinase. *Biomed. Pharmacother.* **2018**, *105*, 320−325.
(25) Boyd, M. R.; Pauli, K. D. Some Practical Considerations and Applications of the National-Cancer-Institute in-Vitro Anticancer Drug Discovery Screen. *Drug Dev. Res.* **1995**, *34*, 91−109.
(26) Jannuzzi, A. T.; Yıldız, M.; Bayrak, N.; Yıldırım, H.; Shilkar, D.; Jayaprakash, V.; TuYuN, A. F. Anticancer agents based on Plastoquinone analogs with N-phenylpiperazine: Structure-activity relationship and mechanism of action in breast cancer cells. *Chem.-Biol. Interact.* **2021**, *349*, No. 109673.
(27) Pelicano, H.; Zhang, W.; Liu, J.; Hammoudi, N.; Dai, J.; Xu, R. H.; Pusztai, L.; Huang, P. Mitochondrial dysfunction in some triple-negative breast cancer cell lines: role of mTOR pathway and therapeutic potential. *Breast Cancer Res.* **2014**, *16*, No. 434.
(28) (a) Pfeffer, C. M.; Singh, A. T. K. Apoptosis: A Target for Anticancer Therapy. *Int. J. Mol. Sci.* **2018**, *19*, 448. (b) Fulda, S.; Debatin, K. M. Extrinsic versus intrinsic apoptosis pathways in anticancer chemotherapy. *Oncogene* **2006**, *25*, 4798−4811.
(29) Gusakov, E. A.; Topchu, I. A.; Mazitova, A. M.; Dorogan, I. V.; Bulatov, E. R.; Serebriiskii, I. G.; Abramova, Z. I.; Tupaeva, I. O.; Demidov, O. P.; Toan, D. N.; et al. Design, synthesis and biological evaluation of 2-quinolyl-1,3-tropolone derivatives as new anti-cancer agents. *RSC Adv.* **2021**, *11*, 4555−4571.
(30) Abotaleb, M.; Kubatka, P.; Caprnda, M.; Varghese, E.; Zolakova, B.; Zubor, P.; Opatrilova, R.; Kruzliak, P.; Stefanicka, P.; Büsselberg, D. Chemotherapeutic agents for the treatment of metastatic breast cancer: An update. *Biomed. Pharmacother.* **2018**, *101*, 458−477.
(31) Lüpertz, R.; Wätjen, W.; Kahl, R.; Chovolou, Y. Dose- and time-dependent effects of doxorubicin on cytotoxicity, cell cycle and apoptotic cell death in human colon cancer cells. *Toxicology* **2010**, *271*, 115−121.
(32) DiPaola, R. S. To arrest or not to G(2)-M Cell-cycle arrest: commentary re: A. K. Tyagi et al., Silibinin strongly synergizes human prostate carcinoma DU145 cells to doxorubicin-induced growth inhibition, G(2)-M arrest, and apoptosis. *Clin. Cancer Res.* **2002**, *8*, 3311−3314.
(33) Redza-Dutordoir, M.; Averill-Bates, D. A. Activation of apoptosis signalling pathways by reactive oxygen species. *Biochim. Biophys. Acta, Mol. Cell Res.* **2016**, *1863*, 2977−2992.
(34) Gfeller, D.; Michielin, O.; Zoete, V. Shaping the interaction landscape of bioactive molecules. *Bioinformatics* **2013**, *29*, 3073−3079.
(35) Shin, Y.; Chen, W.; Habel, J.; Duckett, D.; Ling, Y. Y.; Koenig, M.; He, Y.; Vojkovsky, T.; LoGrasso, P.; Kamenecka, T. M. Synthesis and SAR of piperazine amides as novel c-jun N-terminal kinase (JNK) inhibitors. *Bioorg. Med. Chem. Lett.* **2009**, *19*, 3344−3347.
(36) Zoete, V.; Daina, A.; Bovigny, C.; Michielin, O. SwissSimilarity: A Web Tool for Low to Ultra High Throughput Ligand-Based Virtual Screening. *J. Chem. Inf. Model.* **2016**, *56*, 1399−1404.
(37) Teague, S. J.; Davis, A. M.; Leeson, P. D.; Oprea, T. The Design of Leadlike Combinatorial Libraries. *Angew. Chem., Int. Ed.* **1999**, *38*, 3743−3748.
(38) Lipinski, C. A.; Lombardo, F.; Dominy, B. W.; Feeney, P. J. Experimental and computational approaches to estimate solubility and permeability in drug discovery and development settings. *Adv. Drug Delivery Rev.* **2001**, *46*, 3−26.
(39) Ghose, A. K.; Viswanadhan, V. N.; Wendoloski, J. J. A knowledge-based approach in designing combinatorial or medicinal chemistry libraries for drug discovery. 1. A qualitative and quantitative characterization of known drug databases. *J. Comb. Chem.* **1999**, *1*, 55−68.
(40) Veber, D. F.; Johnson, S. R.; Cheng, H.-Y.; Smith, B. R.; Ward, K. W.; Kopple, K. D. Molecular Properties That Influence the Oral Bioavailability of Drug Candidates. *J. Med. Chem.* **2002**, *45*, 2615−2623.
(41) Egan, W. J.; Merz, K. M., Jr.; Baldwin, J. J. Prediction of drug absorption using multivariate statistics. *J. Med. Chem.* **2000**, *43*, 3867−3877.
(42) Muegge, I.; Heald, S. L.; Brittelli, D. Simple Selection Criteria for Drug-like Chemical Matter. *J. Med. Chem.* **2001**, *44*, 1841−1846.
(43) (a) Monks, A.; Scudiero, D.; Skehan, P.; Shoemaker, R.; Paull, K.; Vistica, D.; Hose, C.; Langley, J.; Cronise, P.; Vaigrowolff, A.; et al. Feasibility of a High-Flux Anticancer Drug Screen Using a Diverse Panel of Cultured Human Tumor-Cell Lines. *J. Natl. Cancer Inst.* **1991**, *83*, 757−766. (b) Grever, M. R.; Schepartz, S. A.; Chabner, B. A. The National-Cancer-Institute - Cancer Drug Discovery and Development Program. *Semin. Oncol.* **1992**, *19*, 622−638.
(44) Skehan, P.; Storeng, R.; Scudiero, D.; Monks, A.; McMahon, J.; Vistica, D.; Warren, J. T.; Bokesch, H.; Kenney, S.; Boyd, M. R. New colorimetric cytotoxicity assay for anticancer-drug screening. *J. Natl. Cancer Inst.* **1990**, *82*, 1107−1112.
(45) (a) Tateishi, H.; Tateishi, M.; Radwan, M. O.; Masunaga, T.; Kawatashiro, K.; Oba, Y.; Oyama, M.; Inoue-Kitahashi, N.; Fujita, M.; Okamoto, Y.; Otsuka, M. A New Inhibitor of ADAM17 Composed of a Zinc-Binding Dithiol Moiety and a Specificity Pocket-Binding Appendage. *Chem. Pharm. Bull.* **2021**, *69*, 1123−1130. (b) Radwan, M. O.; Takaya, D.; Koga, R.; Iwamaru, K.; Tateishi, H.; Ali, T. F. S.; Takaori-Kondo, A.; Otsuka, M.; Honma, T.; Fujita, M. Interruption of Vif/Elongin C interaction: In silico and experimental elucidation of the underlying molecular mechanism of benzimidazole-based APOBEC3G stabilizers. *Bioorg. Med. Chem.* **2020**, *28*, 115409.
(46) Mingle, D.; Ospanov, M.; Radwan, M. O.; Ashpole, N.; Otsuka, M.; Ross, S. A.; Walker, L. A.; Shilabin, A. G.; Ibrahim, M. A. First in class (S,E)-11-[2-(arylmethylene)hydrazono]-PBD analogs as selective CB2 modulators targeting neurodegenerative disorders. *Med. Chem. Res.* **2021**, *30*, 98−108.
(47) Daina, A.; Michielin, O.; Zoete, V. SwissADME: a free web tool to evaluate pharmacokinetics, drug-likeness and medicinal chemistry friendliness of small molecules. *Sci. Rep.* **2017**, *7*, No. 42717.

https://doi.org/10.1021/acsomega.2c03428
ACS Omega 2022, 7, 30250−30264